

# Interactions between the Non-ionic Surfactant C<sub>12</sub>E<sub>5</sub> and Poly(ethylene oxide) Studied Using Dynamic Light Scattering and Fluorescence Quenching

Eloi Feitosa,<sup>†</sup> Wyn Brown,\* and Per Hansson

Department of Physical Chemistry, University of Uppsala, Box 532,  
751 21 Uppsala, Sweden

Received April 17, 1995; Revised Manuscript Received September 22, 1995<sup>®</sup>

**ABSTRACT:** Dynamic light scattering measurements have been made to elucidate changes in the coil conformation of a high molecular weight poly(ethylene oxide) (PEO) fraction when the non-ionic surfactant C<sub>12</sub>E<sub>5</sub> is present in dilute solutions. The measurements were made at 20 °C as functions of (a) the C<sub>12</sub>E<sub>5</sub> concentration at constant PEO concentration, (b) the PEO concentration at constant C<sub>12</sub>E<sub>5</sub> concentration, and (c) the C<sub>12</sub>E<sub>5</sub>/PEO concentration ratio. The influence of temperature on the interactions in terms of the relaxation time distributions was also examined up to the cloud point. It was found that when the C<sub>12</sub>E<sub>5</sub>/PEO weight ratio was > 2 and when the temperature was > 14 °C, the correlation functions became bimodal with well-separated components. The fast mode derives from individual surfactant micelles which are present in the solution at high number density. The appearance of the slow mode, which dominates the scattering, is interpreted as resulting from the formation of micellar clusters due to an excluded-volume effect when the high molar mass ( $M = 6 \times 10^5$ ) PEO is added to the surfactant solution. It is shown that the micellar clusters form within the PEO coils and lead to a progressive swelling of the latter for steric reasons. The dimensions of the PEO/C<sub>12</sub>E<sub>5</sub> complex increase with increasing surfactant concentration to a value of  $R_H \approx 94$  nm ( $R_g \approx 208$  nm) at  $C_{C_{12}E_5} = 3.5\%$ . Fluorescence quenching measurements show that the average aggregation number of C<sub>12</sub>E<sub>5</sub> increases significantly on addition of the high molar mass PEO. With increasing temperature toward the cloud point the clusters increase in number density and/or become larger. The cloud point is substantially lower than that for C<sub>12</sub>E<sub>5</sub> in water solution and is strongly dependent on the PEO concentration.

## Introduction

The interactions between surfactants and polymers are a subject of great interest which also has important technological implications; see, for example, recent reviews.<sup>1–3</sup> Adding a surfactant to a polymer solution with formation of a surfactant/polymer complex can substantially alter the physical properties of the starting polymer, for example, by imparting polyelectrolyte characteristics to a neutral polymer such as poly(ethylene oxide) (PEO) by addition of SDS (see, for example, refs 4 and 5) or by partial neutralization of the intrinsic polyelectrolyte charge by adding CTAB of opposite charge to solutions of sodium polystyrene sulfonate.<sup>6,7</sup> Pronounced changes in coil conformation occur in these cases. It is generally accepted<sup>1–3</sup> that an ionic surfactant interacts with the polymer chain as small micellar aggregates, which are first formed at the critical aggregation concentration (cac); the latter is substantially lower than the critical micelle concentration (cmc) of the pure surfactant in solution. The interactions may involve electrostatic, hydrophobic, and steric interactions, which together serve to considerably modify the overall coil conformation of the original polymer chain. Ricka and co-workers<sup>8</sup> have illustrated this in the case of SDS added to solutions of poly(*N*-isopropylacrylamide) with considerable modification of the coil-to-globule transition. Almost all the prior work has involved addition of a charged surfactant either to a neutral polymer or to a polyelectrolyte. In general, there is a much stronger affinity between anionic surfactants and neutral polymers compared to cationic surfactants and neutral polymers<sup>3</sup>.

There is, however, ambiguous and less well-documented experimental evidence for interactions between

the neutral counterparts. According to the review of Saito,<sup>2</sup> hydrophilic polymers such as poly(vinyl alcohol) (PVA), PEO, and poly(vinylpyrrolidone) (PVP) show no signs of interaction with the polyethoxylated non-ionic surfactants, C<sub>*m*</sub>E<sub>*n*</sub>. However, the latter type of non-ionic surfactants was shown to interact weakly with poly-(carboxylic acids).<sup>2</sup> Subsequently, a number of communications have appeared detailing interactions between uncharged polymers and non-ionic surfactants (see ref 3 for a review). For example, Brackman et al.<sup>9</sup> described microcalorimetric measurements on solutions of poly(propylene oxide) (PPO),  $M = 1000$ , containing the non-ionic surfactant *n*-octyl thioglucoside micelles (OTG). Although the cmc was identical with and without the polymer, the results gave clear evidence for an endothermic interaction between the components.

Winnik<sup>10</sup> studied the interaction between pyrene-labeled hydroxypropyl-cellulose and OTG using fluorescence measurements. From measurements of the ratio of the pyrene monomer emission to the pyrene excimer emission intensity and its changes with surfactant concentration, the author reported the first unambiguous detection of complex formation between neutral polymers and neutral surfactants. Cohen-Addad and di Meglio<sup>11</sup> also described foam stabilization in the C<sub>12</sub>E<sub>5</sub>/PEO system and again the results were interpreted in terms of polymer/surfactant interaction.

Thus, although non-ionic surfactants have the same value for the cmc in the presence of the polymer as in water, in contrast to the considerably lower cac when ionic surfactants interact with uncharged polymers, this need not unequivocally mean the absence of interaction. It probably does mean, however, that the interactions do not involve the same type of specificity in the binding of surfactant micelles to the polymer chain as for example in the PEO/SDS system mentioned above. Nevertheless, the solution properties of the polymeric component may still be strongly changed in the presence

<sup>†</sup> Permanent address: Departamento de Física, IBILCE/UNESP, São José do Rio Preto, SP, Brazil.

<sup>®</sup> Abstract published in *Advance ACS Abstracts*, February 1, 1996.

of the surfactant since, as pointed out by Winnik,<sup>10</sup> polymer/polymer aggregates are disrupted and the conformation of the polymer is modified. Since light scattering measurements provide a non-invasive means of probing conformational changes we chose to apply dynamic light scattering (DLS) and fluorescence quenching measurements to elucidate such changes in the interaction pattern in mixtures of a high molecular weight fraction of PEO and the non-ionic surfactant C<sub>12</sub>E<sub>5</sub> (which itself contains a PEO segment as the hydrophilic entity) in aqueous solution. It will be noted that the binary aqueous solutions of the components are in themselves not straightforward in terms of their solution properties. C<sub>12</sub>E<sub>5</sub> shows a pronounced tendency for micellar growth with both temperature and concentration change while high molar mass PEO almost invariably reveals the presence of clusters in its solutions. As will be discussed below, however, the mixtures in solution display features that are not present in the binary solutions.

## Experimental Section

**Materials.** C<sub>12</sub>E<sub>5</sub> and PEO are from, respectively, Nikko Chemicals, Tokyo, Japan, and Toya Soda, Ltd. Tokyo, Japan, and were used without further purification. PEO has  $M_w = 5.94 \times 10^5$  and  $M_w/M_n = 1.04$ . Solutions were prepared using purified water (Milli-Q plus) and filtered through 0.22- $\mu$ m Millipore filters directly into the scattering ampoules. The results are presented in terms of weight percent (1% w/w is equivalent to  $2.46 \times 10^{-2}$  M for C<sub>12</sub>E<sub>5</sub> and 0.23 M in terms of the PEO monomer). The cmc of C<sub>12</sub>E<sub>5</sub> is  $2.64 \times 10^{-3}\%$  (65  $\mu$ M) at 25 °C.<sup>12</sup>

Clouding temperatures ( $T_c$ ) of the PEO/C<sub>12</sub>E<sub>5</sub> mixtures were measured by slowly heating the sample in a thermostat and visually observing the sharp demixing at various compositions.

**Dynamic Light Scattering.** Polarized (VV) DLS measurements, in the self-beating (homodyne) mode, were made using a 633 nm He–Ne laser and detector optics employing an ITT FW130 photomultiplier, the output of which was digitized by an ALV-PM-PD amplifier–discriminator. The signal analyzer was an ALV-5000 digital multiple-tau correlator, Langen GmbH, with 288 exponentially spaced channels. It has a minimum real-time sampling time of 0.2  $\mu$ s and a maximum of  $\sim 100$  s. The intensity autocorrelation function,  $g^{(2)}(t)$ , was measured at different angles. The scattering cells (10 mL sealed cylindrical ampoules) were immersed in a large-diameter thermostated bath of index-matching liquid (decalin). The temperature was controlled to within  $\pm 0.02$  °C.

**Data Analysis.** The DLS data were analyzed by nonlinear regression procedures. The function fitted was the intensity autocorrelation function described as

$$g^{(2)}(t) - 1 = \beta |g^{(1)}(t)|^2 \quad (1)$$

where  $\beta$  is a nonideality factor accounting for deviation from ideal correlation.  $g^{(1)}(t)$  can be written as the Laplace transform of the distribution of relaxation rates,  $G(\Gamma)$ :

$$g^{(1)}(t) = \int_0^\infty G(\Gamma) \exp(-\Gamma t) d\Gamma \quad (2)$$

For relaxation times,  $\tau$ , this is expressed

$$g^{(1)}(t) = \int_{-\infty}^\infty \tau A(\tau) \exp(-t/\tau) d \ln \tau \quad (3)$$

where  $t$  is the lag time.  $\tau A(\tau)$  was obtained by inverse Laplace transformation (ILT) using a constrained regularization calculation algorithm called REPES as incorporated in the analysis package GENDIST.<sup>14</sup> This algorithm directly minimizes the sum of the squared differences between experimental and calculated  $g^{(2)}(t)$  functions. It allows the selection of a smoothing parameter “probability to reject” ( $P$ ). The higher the  $P$ , the greater the smoothing.

The choice of  $P$  was optimized for each inversion although the initial value of  $P = 0.5$  was chosen as standard in the analyses. Diffusion coefficients are calculated from the ILT moments as  $D = (\Gamma/q^2)_{q \rightarrow 0}$ , where  $q$  is the magnitude of the scattering vector.

**Time-Resolved Fluorescence Quenching (TRFQ).** Fluorescence decay data were collected with the single-photon-counting technique. A detailed description of the experimental technique and equipment used is given elsewhere.<sup>6</sup> All measurements were performed in equilibrium with air. Pyrene and dimethylbenzophenone were used as probe and quencher, respectively.

The TRFQ data were fitted to the Infelta–Tachiya equation:<sup>15,16</sup>

$$F(t) = A_1 \exp[-A_2 t + A_3 \{\exp(-A_4 t) - 1\}] \quad (4)$$

where  $F(t)$  describes the time evolution of the fluorescence intensity. When probe and quencher are stationary in the micelles during the lifetime of the probe, the parameters  $A_1 - A_4$  can be interpreted as follows:  $A_1 = F(0)$ ,  $A_2 = 1/\tau_0$ ,  $A_3 = \langle n \rangle$ , and  $A_4 = k_q$ .  $F(0)$  is the intensity at zero time,  $\tau_0$  the natural lifetime of the probe,  $\langle n \rangle$  the average number of quenchers in a micelle, and  $k_q$  the intramicellar quasi-first-order quenching constant. This interpretation demands a Poisson distribution of the quencher over the micelles. In the fitting procedure, the  $A_2$  parameter was fixed to  $1/\tau_0$ , as estimated from separate experiments without quencher. The surfactant aggregation number,  $N$ , was calculated from  $C_{s,m}$  and  $C_{q,m}$ , the concentration of surfactant and quencher in micelles, respectively, and  $\langle n \rangle$  using the relationship

$$N = \langle n \rangle C_{s,m} / C_{q,m} \quad (5)$$

At the surfactant concentrations used in this study, the free concentrations of surfactant and quencher are negligible. Thus,  $C_{s,m}$  and  $C_{q,m}$  can be replaced by the total concentration of surfactant and quencher, respectively. The free concentration of the probe is also completely negligible.

## Results and Discussion

**Binary Systems (a) C<sub>12</sub>E<sub>5</sub>/Water.** Figure 1a shows a typical correlation function and an ILT relaxation time distribution for C<sub>12</sub>E<sub>5</sub> in water at 20 °C at a concentration of 0.5% (w/w). The correlogram is very close to a single exponential, although a small-amplitude faster component is present. The evaluated relaxation rate ( $\Gamma$ ) is linearly dependent on  $q^2$  demonstrating a diffusive process.

Figure 1b shows the diffusion coefficients for C<sub>12</sub>E<sub>5</sub> as a function of concentration at 20 °C. The strong initial decrease in the mutual diffusion coefficient  $D$  has been described earlier<sup>13,17,18</sup> and has also been observed in pulsed-field gradient (PFG) NMR experiments.<sup>17</sup> Similar trends have been also noted for other non-ionic surfactants (C<sub>12</sub>E<sub>7</sub> and C<sub>12</sub>E<sub>8</sub>) with the depth of the minimum diminishing as the ethylene oxide moiety increased in length. Since the mutual diffusion coefficient is related to the thermodynamic interaction in the system, it was proposed in refs 13 and 18 that there are strong changes in the intermicellar interactions at concentrations in the vicinity of the minimum  $D$  value and that pronounced micellar shape changes occur with concentration change. The initial decrease in  $D$  suggests strong micellar growth over a narrow range of concentration starting at  $c < 1.5\%$ . At concentrations above the minimum in  $D$  where the semidilute concentration range is entered, the long micelles give rise to a large excluded-volume effect and the slope is strongly positive.

An approximate value for  $R_H$  can be obtained by extrapolating the curved portion in Figure 1b to infinite dilution. This gives 11.9 nm for the main micellar

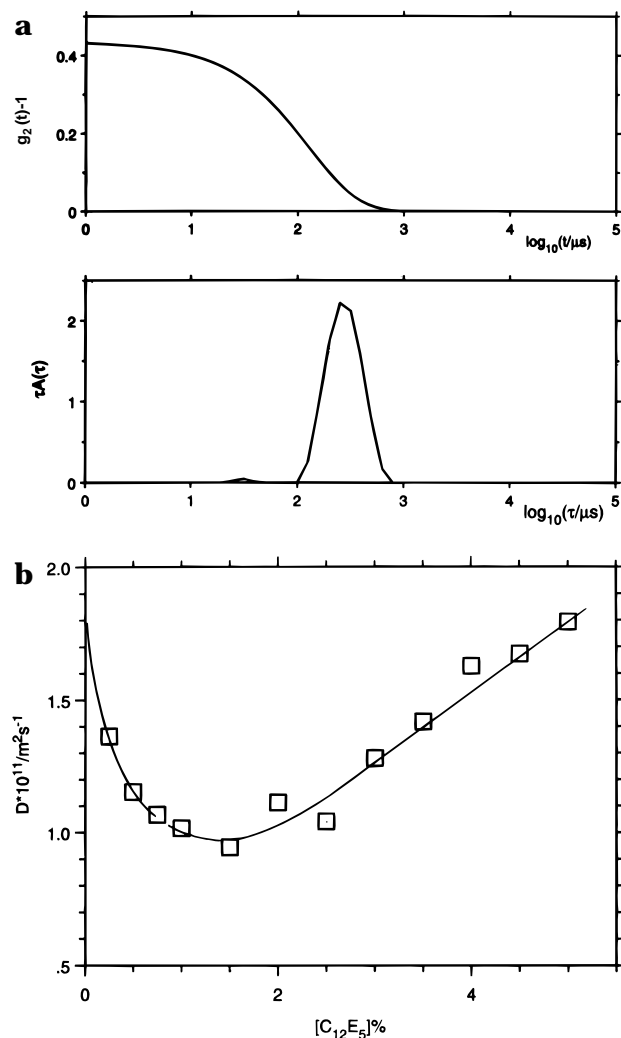


**Figure 1.** (a, top) Autocorrelation function ( $g^2(t)$ ) (top) and ILT relaxation time distribution (bottom) for a 0.5% solution of C<sub>12</sub>E<sub>5</sub> at 20 °C; measurements at  $\theta = 90^\circ$ . (b, bottom) Diffusion coefficients for C<sub>12</sub>E<sub>5</sub> as a function of  $C$  in the for C<sub>12</sub>E<sub>5</sub> solutions; 20 °C.

component (using  $D_0 = 1.8 \times 10^{-11} \text{ m}^2 \text{ s}^{-1}$  at 20 °C). PFG NMR data gave  $R_H \approx 7 \text{ nm}$  using the data summarized in Figure 3 of ref 13. The lower value is probably the result of considerable polydispersity since  $D$  from PFG NMR approximates a number-averaged quantity and DLS the higher  $z$ -averaged quantity. The DLS value agrees, however, with that previously given (12 nm) in ref 13. (Extrapolation of the present C<sub>12</sub>E<sub>5</sub> data at 20 °C to infinite dilution from the linear part of the curve at the higher concentrations, on the other hand, would give  $R_H \approx 40 \text{ nm}$ , a value that is unrealistically large for the micellar radius.) Although the extrapolated value is uncertain,  $R_H = 12 \text{ nm}$  will be used for comparisons with the dimensions of the free micelles in the polymer/surfactant mixed systems. It was concluded in ref 13 that below 10 °C the C<sub>12</sub>E<sub>5</sub> micelles are large and rodlike. At  $\sim 15^\circ \text{C}$ , the micelles are substantially smaller than at low temperatures but then grow with increasing temperature. Thus the minimum in Figure 1b is displaced to lower concentration with increasing temperature. Kato et al.<sup>18</sup> also showed that the correlation length increases with increasing temperature, demonstrating micellar growth.

**(b) PEO/Water.** Figure 2a shows a typical correlation function for PEO in water at  $c = 0.5\%$  and the resulting ILT relaxation time distribution. This is

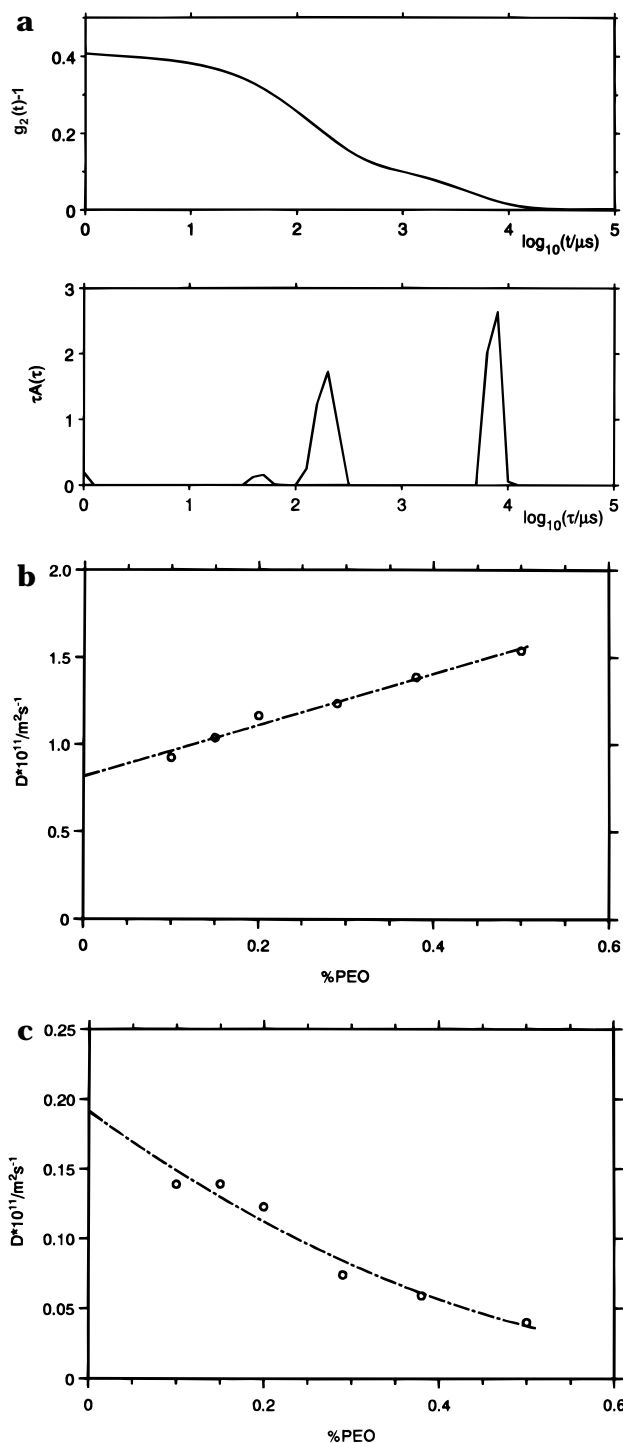


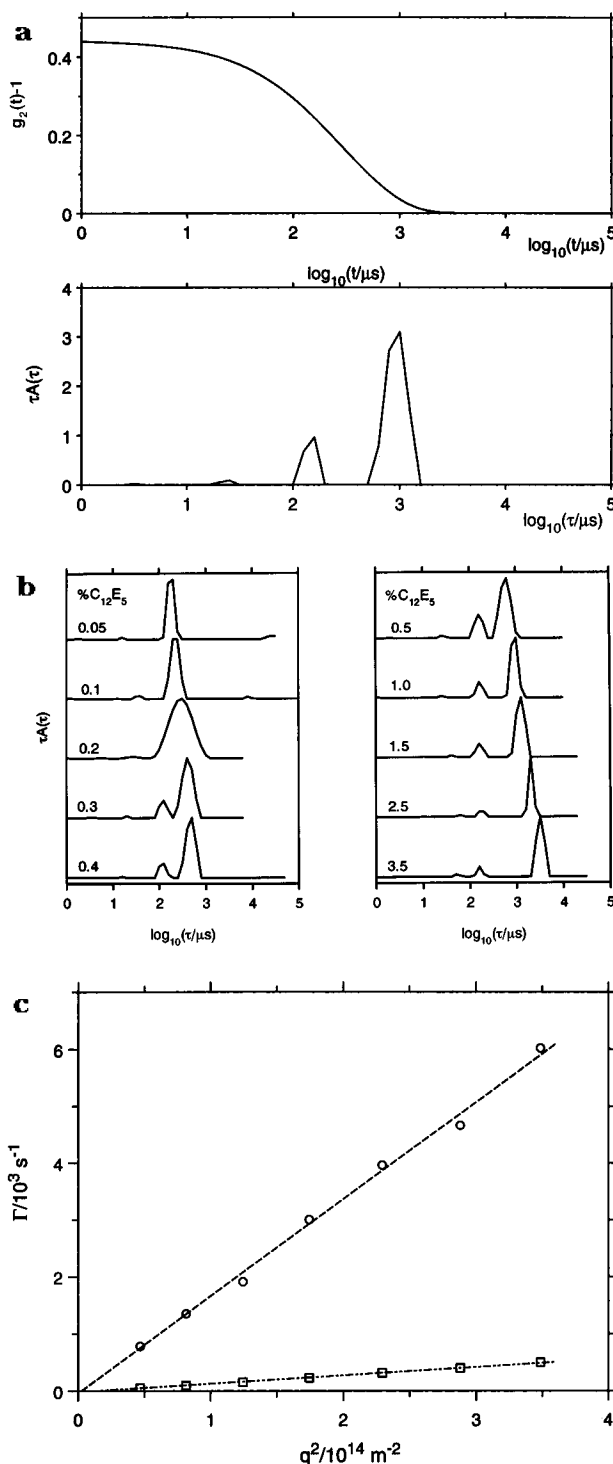
**Figure 2.** (a, top) Autocorrelation function (upper) and (ILT) distribution (lower) for PEO ( $M_w = 5.9 \times 10^5$ ) at  $c = 0.5\%$  and 20 °C;  $\theta = 90^\circ$ . (b, middle) Diffusion coefficients for the fast PEO mode (single coil) as a function of concentration at 20 °C. (c, bottom) Concentration dependence of the slow PEO mode at 20 °C.

bimodal. Both modes are diffusive, as was established by the linear dependence of the relaxation rate ( $\Gamma$ ) on  $q^2$ . The slow “cluster” mode has been considered characteristic of dilute solutions of PEO in both water and non-aqueous solvents.<sup>19</sup> However, recent papers<sup>20,21</sup> have reported that it is possible to prepare aggregate-free PEO solutions in water by the use of very “tight” filters, e.g., 0.02- or 0.05- $\mu\text{m}$  pore size, whereas the usually employed 0.22- $\mu\text{m}$  filters do not remove this component.

Diffusion coefficients are shown in Figure 2b for the fast mode. The  $D_0$  value corresponds to  $R_H = 26.3$  nm (20 °C) obtained using the Stokes–Einstein equation together with the solvent viscosity. The fast mode is thus concluded to correspond to the PEO single coil. We estimate an approximate radius of gyration ( $R_g$ ) from the intrinsic viscosity using the well-known Flory–Fox expression for the intrinsic viscosity of flexible chains in dilute solution. For this fraction ( $[\eta] = 418$  mL g<sup>-1</sup> gives  $R_g = 43$  nm),  $R_g/R_H = 1.74$ . The latter ratio is typical of a flexible Gaussian coil,<sup>22</sup> which shows that a single chain is involved. The slow cluster mode shown in Figure 2c gives a  $D_0$  value that corresponds to a value of  $R_H = 112$  nm.

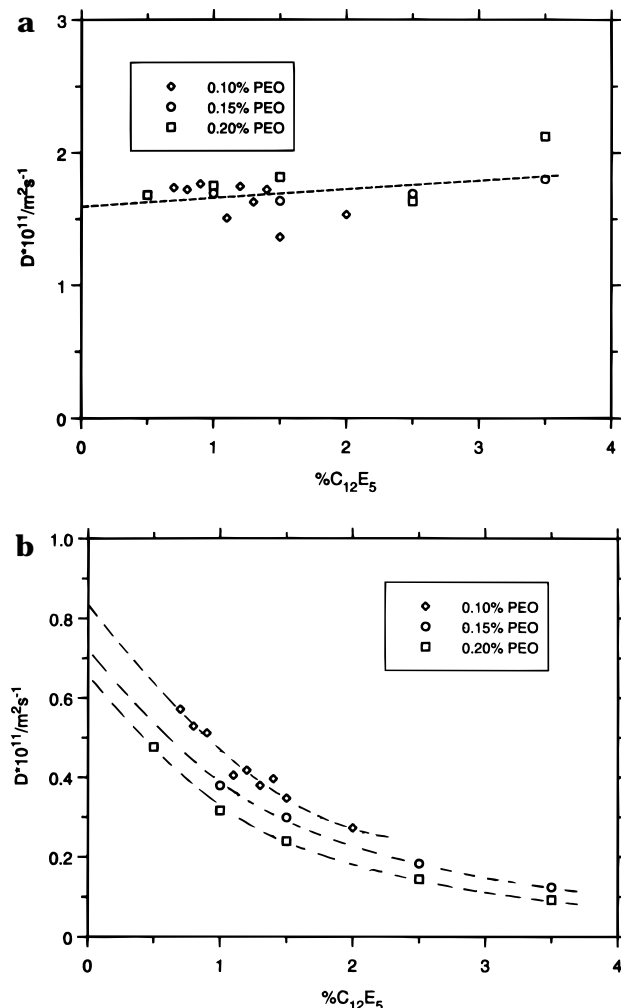
**Ternary Solutions: C<sub>12</sub>E<sub>5</sub>/PEO/Water.** Figure 3a shows a typical correlation function and an ILT relaxation time distribution for a solution containing 0.5% of C<sub>12</sub>E<sub>5</sub> and PEO at 20 °C. A bimodal distribution is first observed above a certain minimum concentration of surfactant for a given concentration of PEO. The progressive change in the distributions with increase of the surfactant concentration is illustrated in Figure 3b for a constant  $c_{\text{PEO}} = 0.2\%$ . Above  $\sim 0.2\%$  C<sub>12</sub>E<sub>5</sub>, the distributions become bimodal. (It is important to note that for the binary surfactant solution at this temperature the relaxation time distributions are unimodal with no trace of a slower mode present.) The fast mode has an approximately constant relaxation time while the slow mode is successively displaced to longer relaxation times. Both modes are diffusive as shown by the plots of  $\Gamma$  versus  $q^2$ , passing through the origin as depicted in Figure 3c. It is also important to note that when C<sub>12</sub>E<sub>5</sub> has been added to a PEO solution at a very low concentration, the cluster component noted above in the binary PEO solution is absent (Figure 2a). The multi-chain aggregates of PEO probably form owing to residual hydrophobic impurities in the polymer deriving from the preparation of the fractions.<sup>21</sup> As will be pointed out below in the discussion of the ternary systems, addition of the surfactant removes the “cluster” peak in PEO solutions, probably because these hydrophobic impurities are incorporated into the micellar core. Inhibition of polymer cluster formation by surfactant was previously noted<sup>7</sup> for poly(styrene sulfonate) in the presence of the ionic surfactant CTAB. In this latter case, however, the surfactant serves to screen the charge interactions that lead to the aggregate formation, which is a well-known feature in polyelectrolytic solutions.

Figure 4 shows the diffusion coefficients obtained from the distributions in Figure 3b as a function of surfactant concentration at three constant levels of PEO concentration. The relaxation time of the fast mode is approximately constant with change in the PEO concentration, and the concentration dependence is small. From the infinite dilution value, it is estimated that the free micelles thus have an approximate size of  $R_H = 12$  nm which agrees well with the value for the surfactant in binary solution. These data scatter strongly, probably owing to poorer resolution due to partial overlap of the ILT peaks. The relaxation time for the slower mode increases with increasing C<sub>12</sub>E<sub>5</sub>. The intercepts at  $c_{\text{C}_{12}\text{E}_5} \rightarrow 0$  yield the apparent hydrodynamic radii of the slow mode, i.e., the radius at a given constant value of PEO concentration. The approximate values estimated by extrapolating to zero surfactant concentrations are as follows: 0.1% PEO, 25.8 nm; 0.15% PEO, 30.6 nm, and 0.2% PEO, 34.8 nm.



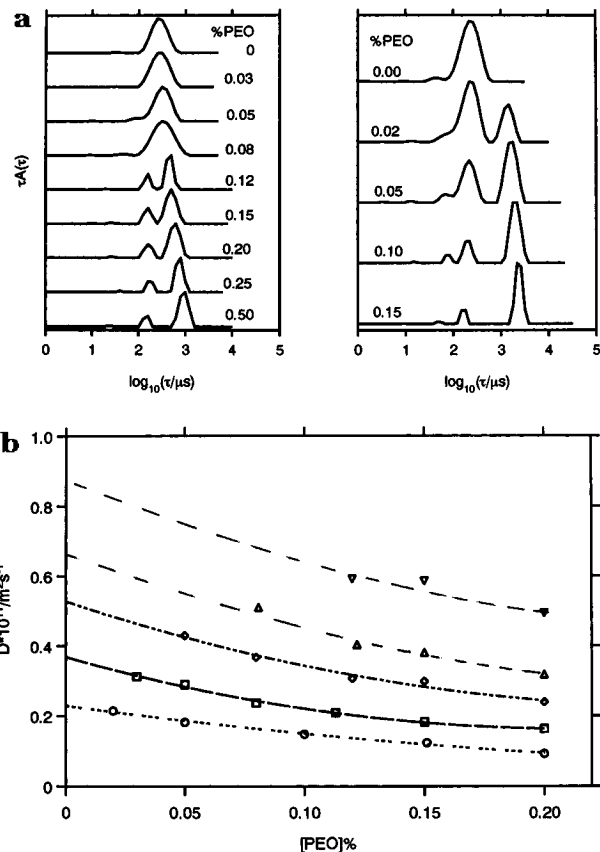
**Figure 3.** (a, top) Autocorrelation function (upper) and (ILT) distribution (lower) for a C<sub>12</sub>E<sub>5</sub>/PEO mixture in solution at equal concentrations of 0.5%; measurements at 20 °C and  $\theta = 90^\circ$ . (b, middle) ILT relaxation time distributions for constant PEO concentration (0.2%) with successive increase of C<sub>12</sub>E<sub>5</sub> concentration at 20 °C. (c, bottom) Dependence of the relaxation rate ( $\Gamma$ ) versus the square of the scattering vector ( $q^2$ ) for the ternary system (2.5% C<sub>12</sub>E<sub>5</sub>, 0.2% PEO; 20 °C).

Figure 5 shows analogous relaxation time distributions for solutions in which the surfactant concentration is held constant and the PEO concentration is increased. In Figure 5a, left, with  $c_{\text{C}_{12}\text{E}_5} = 0.5\%$ , the ILT distributions become bimodal above  $c_{\text{PEO}} \approx 0.08\%$ . The slow component again becomes progressively slower in relaxation time, whereas the fast component has an approximately constant value. At  $c_{\text{C}_{12}\text{E}_5} = 3.5\%$  (Figure



**Figure 4.** (a, top) Variation of the diffusion coefficients for the fast mode with increasing surfactant concentration at constant PEO concentrations of 0.1, 0.15, and 0.2% and 20 °C. (b, bottom) Diffusion coefficients for the complex mode as a function of surfactant concentration at constant PEO concentrations at 20 °C.

5a, right), splitting into two modes has already occurred below  $c_{\text{PEO}} = 0.02\%$ . The results reported in the earlier paper,<sup>13</sup> and discussed above with regard to the binary C<sub>12</sub>E<sub>5</sub>/water solutions, show that this surfactant has a strong tendency to micellar growth as functions of both concentration and temperature. Although, as pointed out below in the discussion of the temperature dependence, C<sub>12</sub>E<sub>5</sub> itself in aqueous solution shows no tendency for micellar cluster formation all the way up to the cloud point, it was shown in ref 13 that other non-ionic micellar systems display a low-intensity component with long relaxation time. The relative amplitude of this cluster peak increases as the cloud point is approached, indicating a sensitive equilibrium between the individual micelles and their clusters. The analogous cluster peak is not observed with C<sub>12</sub>E<sub>5</sub> owing to the proximity of the overlap point (the overlap concentration is low ( $\sim 1.5\%$ )). Thus it is to be expected that the addition of high molecular weight PEO with an associated large excluded volume to the system will displace such an equilibrium and induce cluster formation of the micellar component. Coupled with the well-known weak or negligible energetic interactions between non-ionic surfactants and neutral polymers, this interpretation means that the effect is primarily entropic. A plausible interpretation of the data for the slow mode



**Figure 5.** (a, top) ILT relaxation time distributions at two levels of C<sub>12</sub>E<sub>5</sub> concentration: left, 0.5%; right 3.5%. The PEO concentration is changed progressively as shown. The slow mode corresponds to the PEO/C<sub>12</sub>E<sub>5</sub> complex and the fast component to free C<sub>12</sub>E<sub>5</sub> micelles. (b, bottom) Diffusion coefficients for the slow mode as a function of constant C<sub>12</sub>E<sub>5</sub> concentration as shown, plotted versus PEO concentration in the dilute regime. Surfactant concentrations are (from top to bottom): 0.5, 1.0, 1.5, 2.5, and 3.5%.

depicted in Figures 4b and 5a is thus that the micelles are induced to form clusters by the excluded-volume effect of the large ( $R_g \approx 43$  nm) PEO coils. As will be pointed out below, the clusters are apparently sited within the PEO coils with formation of a PEO/C<sub>12</sub>E<sub>5</sub> complex. The scattering from the latter component then dominates the correlogram and much exceeds that from the free surfactant micelles at the concentrations used.

The fast mode, which separates above  $c > 0.2\%$  C<sub>12</sub>E<sub>5</sub> in Figure 3b and  $c > 0.08\%$  PEO in Figure 5a, clearly corresponds to free C<sub>12</sub>E<sub>5</sub> micelles which coexist in the solution with the PEO/C<sub>12</sub>E<sub>5</sub> complex as deduced from the changes in the hydrodynamic radius. Figure 5b shows diffusion coefficients for the slow mode as a function of PEO concentration, where the data have been obtained by holding the surfactant concentration constant at different levels of C<sub>12</sub>E<sub>5</sub> between 0.5 and 3.5%. The PEO concentration range was selected so that  $c < c^*$ , where the overlap concentration for this PEO fraction was estimated using  $c^* = 1/[\eta] = 0.24\%$ .<sup>27</sup>

Conventionally, the concentration dependence of the diffusion coefficient in binary polymeric dilute solutions is given by

$$D = D_0(1 + k_D c + \dots) \quad (6)$$

where  $k_D$  is related to the second virial coefficient, i.e., to the pair interaction potential, by  $k_D = 2A_2M - k_f - 2v_2$ ;  $k_f$  describes the concentration dependence of the

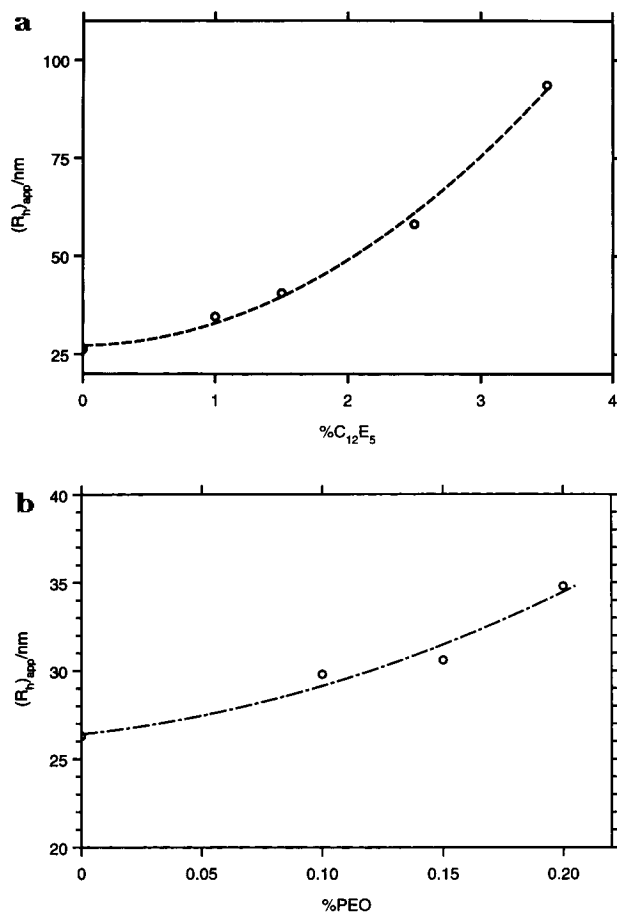


**Figure 6.** (a, top) Apparent hydrodynamic radius obtained at zero PEO concentration as a function of  $C_{12}E_5$  concentration; 20 °C. (b, bottom) Apparent hydrodynamic radius obtained at zero  $C_{12}E_5$  concentration as a function of PEO concentration; 20 °C.

friction factor and  $v_2$  is the partial specific volume of the particle. In the presence of PEO, however, the concentration dependences become nonlinear and negative and, in analogy with binary systems, imply attractive interactions between the micellar clusters induced in the system by addition of PEO. This behavior may be contrasted with the positive value of  $k_D$  for the binary PEO solutions shown in Figure 2b. In binary systems, a negative concentration dependence would mean that association or aggregation occurs. Micellar systems are more complex in that extensive changes in size (molecular weight) and shape can take place, depending on the system and the location in the phase diagram. Since, as we shall show below, the PEO/ $C_{12}E_5$  complex grows with increasing concentration of both the components (Figure 6), as well as the temperature, we conclude even in this case that (i) micellar cluster formation is favored, (ii) the cluster size probably increases with increasing concentration, and (iii) the overall PEO/ $C_{12}E_5$  complex as a result also expands with increasing concentration. The negative concentration dependence is also consistent with the strongly lowered cloud point observed for  $C_{12}E_5$  when PEO is present in the solutions in comparison with the pure surfactant at the same concentration—see below. Both  $c$  and  $k_D$  in eq 6 should refer to the PEO/ $C_{12}E_5$  complex, but the complex concentration is inaccessible in the absence of quantitative information on the association. For this reason we do not evaluate  $k_D$ . The structure of the complex is shown to be dependent on the concentration of both components. Thus, it is necessary to suc-

ccefully extrapolate the  $D$  values to infinite dilution with respect to one component, while holding the concentration of the other constant.

Combination of the approximate infinite dilution values for the slow-mode diffusion coefficient at a series of constant  $C_{12}E_5$  concentrations in Figure 5b with the solvent viscosity in the Stokes–Einstein equation gives the  $R_H$  values displayed in Figure 6a. Solvent viscosities are used to derive  $R_H$  since the surfactant micelles overlap at concentrations above the minimum in Figure 1b. Even allowing for a large uncertainty in the values, there is a strong increase in  $(R_H)_{app}$  with increasing surfactant concentration to a value of  $\sim 94$  nm at  $c_{C_{12}E_5} = 3.5\%$ . This value of  $R_H$  corresponds to roughly 370 micelles per complex, assuming dense packing of spherical micelles in a cluster of micelles within a given coil.

Figure 6b shows the  $R_H$  values similarly derived from extrapolation to infinite dilution of diffusion coefficients for the complex mode in Figure 4 at several constant concentrations of PEO. It is noted that there is a weaker dependence of  $(R_H)_{app}$  on PEO concentration than on the  $C_{12}E_5$  concentration. The extrapolations used to obtain the data in Figure 6 are simplified by the comparatively weak dependencies of the slow mode on the concentration of each component. It is important to note, however, that in both Figure 6a and b  $R_H$  starts from a value equal to the size of the single PEO coil ( $\sim 26$  nm) rather than the  $C_{12}E_5$  micellar radius (12 nm). This shows that, although the scattering probably derives mainly from the micellar clusters, the polymer chain also extends with the increasing size of the clusters, i.e., there is a progressive uncoiling of the PEO chain which apparently occurs to accommodate cluster growth, finally yielding a PEO/ $C_{12}E_5$  complex. Presumably, nonspecific interactions between polymer and micelles lead to a preferred environment for the surfactant. This conclusion is substantiated by the increase in the average aggregation number of the  $C_{12}E_5$  micelles in the presence of PEO—see below. Similarly, PPO has been found to uncoil in the presence of OTG by Brackman et al.<sup>9</sup> Thus, the surfactant micelles apparently nucleate, forming clusters of micelles within the polymer coil, with the surfactant micellar cluster surrounded by a meandering PEO chain, rather than a model in which relatively compact PEO coils are interspersed by segregated surfactant clusters. The PEO chain used here has a contour length of the magnitude 2400 nm if a meander conformation is assumed with the chain twisted into an expanded helical form and using a dimension for the ethylene oxide unit of  $\sim 1.8$  Å.<sup>23</sup>

This “coil/cluster” model for the complex is considered reasonable since, as is discussed below, fluorescence quenching measurements show that the average aggregation number increases significantly on adding PEO.

Total intensity measurements on the solutions used to assemble the data in Figure 5b showed that, for the slow mode depicted, there is excess low-angle scattered intensity and the concentration dependence of the reduced scattered intensity is negative and nonlinear. Estimates of  $R_g$  from the initial slope of the reciprocal intensity showed that  $qR_g > 1$  for all angles used; i.e., the data lie outside of the Guinier range. The Debye function

$$P(X) = (2/X^4)[\exp(-X^2) + X^2 - 1] \quad (7)$$

with  $X = qR_g$ , was thus used to evaluate  $R_g$  at each measurement angle, and the values were extrapolated to zero angle. The value of 208 nm was obtained for

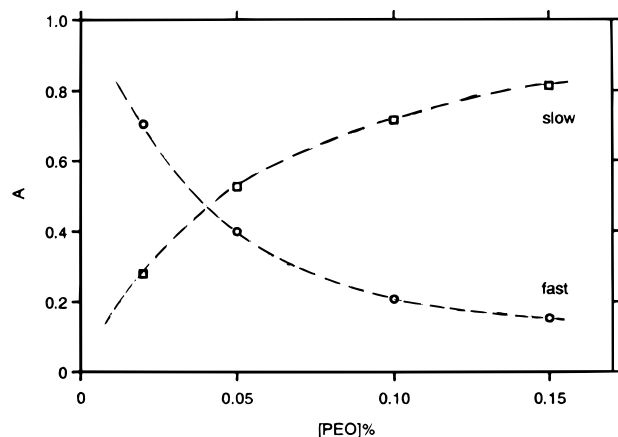


**Figure 7.** Relative amplitudes of the fast and slow modes for the system at constant surfactant concentration of 3.5% as a function of PEO concentration; 20 °C.

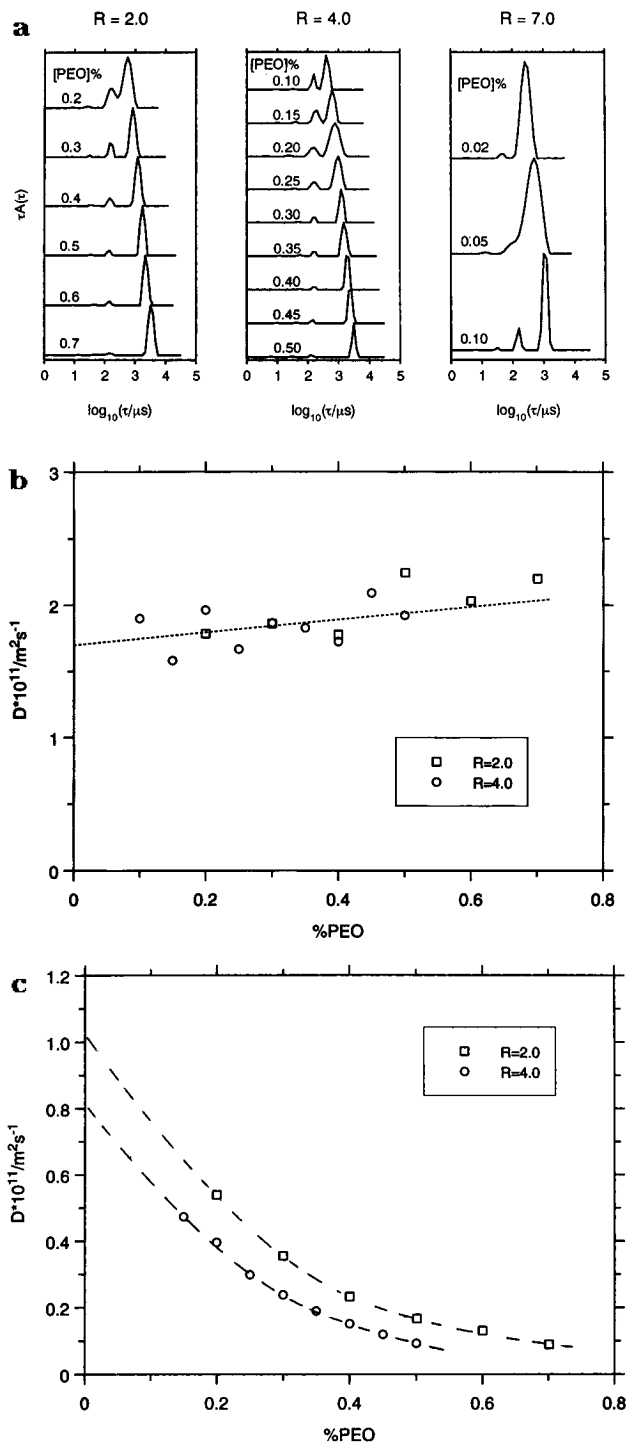
the sample with 3.5% C<sub>12</sub>E<sub>5</sub>. This confirms by an independent measurement that the PEO/C<sub>12</sub>E<sub>5</sub> complex is large, although there is considerable uncertainty in determining a precise value of  $R_g$  in this way.

Figure 7 shows the change in the relative amplitudes of the two modes with change in PEO concentration at constant surfactant concentration. The scattering from the complex dominates the scattering behavior at all but the lowest concentrations of PEO. The scattering intensity from the PEO single coil is very low by comparison with the mixtures.

ILT distributions at constant surfactant/PEO ratio are shown in Figure 8a to complement the data obtained by holding the components fixed in succession. Similar trends are discerned as described above: thus, the ILT distributions are bimodal above a concentration of 0.2% and the relative amplitude of the slow-mode peak increases with increasing concentration. Figure 8b shows the corresponding fast mode diffusion coefficients for surfactant/polymer ratios of 2 and 4. The fast-mode relaxation rate at infinite dilution again corresponds to the hydrodynamic radius of the free micelles, i.e.,  $R_H \approx 12$  nm.

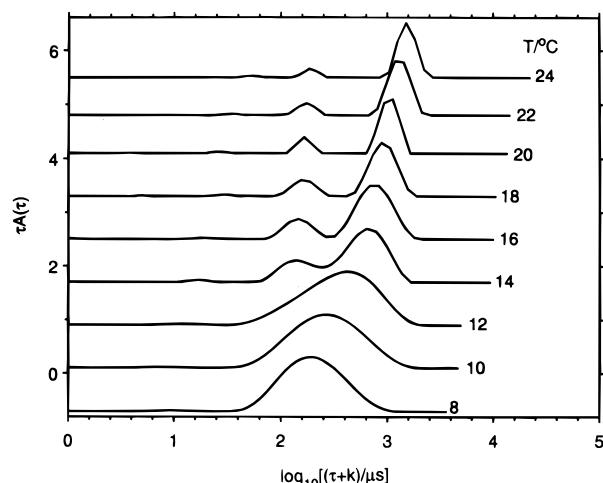
Figure 8c illustrates the strong, non-linear, negative concentration dependence of the cluster mode at the same ratios as in Figure 8b.

Figure 9 presents ILT relaxation time distributions as a function of temperature at equal PEO and C<sub>12</sub>E<sub>5</sub> concentrations of 0.5% (w/w) (i.e.,  $R = 1$ ). The broad single peak at 8–12 °C becomes asymmetric above ~12 °C and at 14 °C has split into two modes. The normalized relaxation time for the fast mode (which again corresponds to  $R_H \approx 12$  nm for the free micelles) changes only weakly with temperature, while the relaxation time for the complex increases more strongly. It is relevant to note that this behavior is strikingly different from that of the binary C<sub>12</sub>E<sub>5</sub>/water system. For the latter, with increasing temperature, the relaxation time distribution remains closely single modal all the way up to the cloud point in the vicinity of 32 °C. There is no indication of the formation of micellar clusters. This contrasts with the complex formation promoted by the presence of high molecular weight PEO at the same temperature in the ternary systems. However, the relaxation time of the single micellar peak increases strongly with temperature. Since the concentration dependence is small, this shows that the C<sub>12</sub>E<sub>5</sub> micelles grow and that this growth continues up to the cloud point due to enhanced attractive interactions. This



**Figure 8.** (a, top) ILT relaxation time distributions at three constant ratios between surfactant and PEO at different PEO concentrations at 20 °C. (b, middle) Dependence of fast diffusion coefficient at constant surfactant/polymer ratios of 2 and 4 on PEO concentration at 20 °C. (c, bottom) Dependence of the complex diffusion coefficient at constant surfactant/PEO ratios  $R = 2$  and 4 on PEO concentration at 20 °C.

behavior is illustrated in Figure 10, which shows that the diffusion coefficients normalized by  $(\eta_0/T)$  have a strong dependence on temperature for both the binary C<sub>12</sub>E<sub>5</sub>/water system and the systems in the additional presence of PEO (a constant ratio surfactant/polymer  $R = 1$  at two total concentrations (0.5 and 1%)). The trend follows those data earlier presented on C<sub>12</sub>E<sub>5</sub> in ref 13, where it was noted that above 15 °C in the binary C<sub>12</sub>E<sub>5</sub>/water system the second virial coefficient from static light scattering decreases monotonically with



**Figure 9.** ILT distributions for  $C_{12}E_5$ /PEO mixtures, ratio  $R = 1$  at a concentration of 0.5% at different temperatures shown. The distributions are shifted on the  $\log \tau$  axis by  $(T/\eta)$ ;  $\theta = 90^\circ$ .

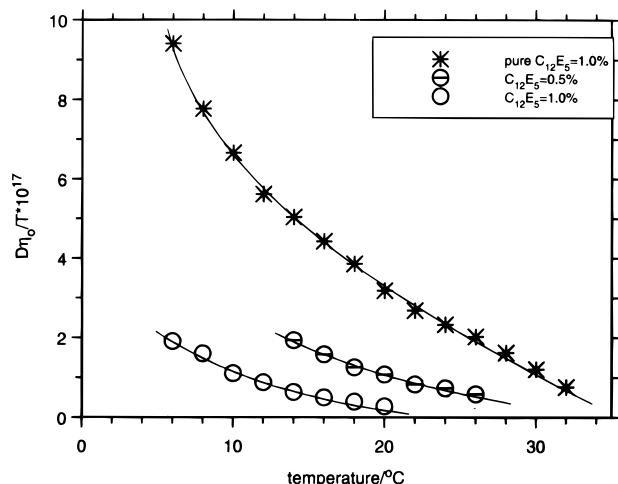


**Figure 10.** Comparison of reduced slow-mode diffusion coefficients ( $D\eta_0/T$ ) versus temperature for pure  $C_{12}E_5$ ,  $c = 1\%$ , and two  $C_{12}E_5$ /PEO mixtures with  $R = 1$  at  $c = 0.5$  and  $1\%$ .

increasing temperature while the weight-average molar mass simultaneously increases as the temperature moves toward the cloud point at  $\sim 32^\circ\text{C}$ . (A similar trend was shown by the other surfactants investigated:  $C_{12}E_8$  and  $C_{12}E_7$ ).

Taken together, the present data establish that the intermicellar attractive interactions are augmented by the presence of PEO and increase strongly with both temperature and concentration. We note here that Piculell and co-workers<sup>24</sup> have recently determined the characteristics of the phase diagram for the  $C_{12}E_5$ /PEO system. The two-phase area increases with increasing temperature. They concluded that the phase behavior is segregative. Wormuth<sup>26</sup> examined the phase behavior of similar amphiphiles (i.e., ethoxylated alcohols) in the presence of PEO. They showed that the miscibility decreases strongly upon increasing the chain lengths of the segments in the amphiphile and also the molar mass of the PEO and found that there are similarities to the phase behavior of two polymers in a solvent.

Figure 11 shows that the scattering intensity of the PEO/ $C_{12}E_5$  complex mode—calculated by apportioning the total intensity using the relative amplitudes of the two modes seen in Figure 9—also increases strongly with increasing temperature. This shows that the mutual interactions between micellar clusters become

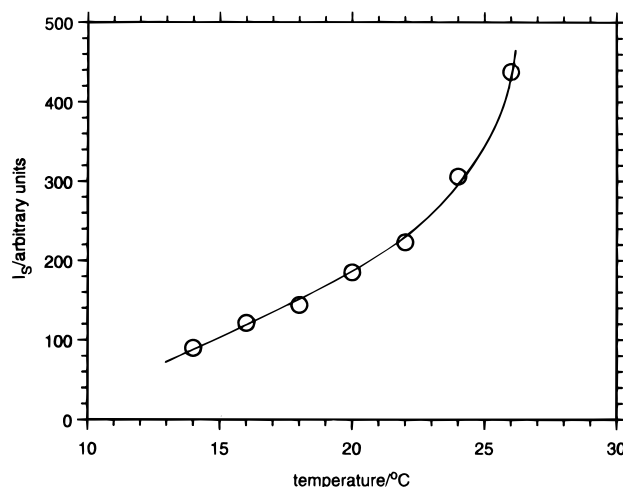


**Figure 11.** Total scattered intensity of the cluster mode versus temperature corresponding to Figure 10.

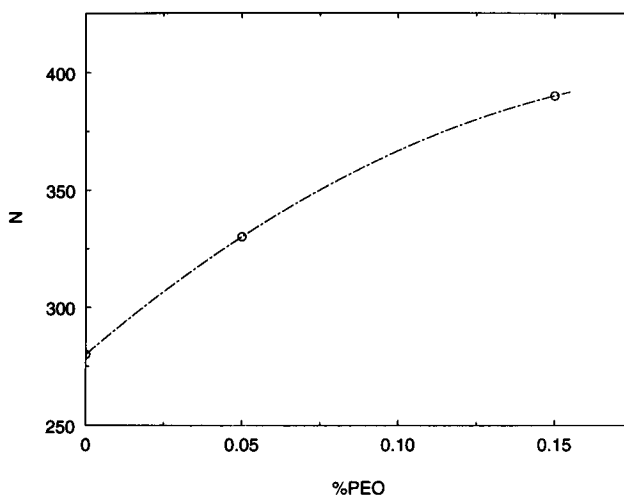


**Figure 12.** Variation of the aggregation number for  $C_{12}E_5$  (0.5%) micelles in the presence of increasing amounts of PEO determined by fluorescence quenching measurements at  $20^\circ\text{C}$ .

progressively more attractive with increasing temperature and that the clusters within the PEO coil grow, as was concluded above from the concentration dependencies in Figure 6.

Fluorescence quenching measurements have been made to ascertain possible changes in the aggregation number ( $N$ ) of  $C_{12}E_5$  on addition of PEO to the solutions. The surfactant concentration and the surfactant-to-quencher ratio were 0.5% and 200, respectively, in all three samples.  $\langle n \rangle (A_3)$  was estimated to be 1.4, 1.7, and 1.9 at PEO concentrations of 0, 0.05, and 0.15, respectively. The quality of the fit was acceptable (reduced  $\chi^2$ , 1.1–1.2). The results in Figure 12 show that there is a significant increase in  $N$  with increasing PEO concentration. The aggregation numbers are quite large. This is expected for this surfactant at  $20^\circ\text{C}$ . The TRFQ data were analyzed with the assumption of no migration of the quencher ( $A_2$  fixed). The time window for the experiment was not enough for the quenched decays to completely develop into the stationary state characteristic of quenching in small micelles. We cannot, therefore, rule out the possibility of migration of the quencher. An analysis of the data with a model that allows for migration ( $A_2$  as a free parameter) gave somewhat smaller aggregation numbers, but the trend was the same as in Figure 12. The fluorescence lifetime for pyrene (solutions in equilibrium with air) was 185 ns at all PEO concentrations used. The quenching rate



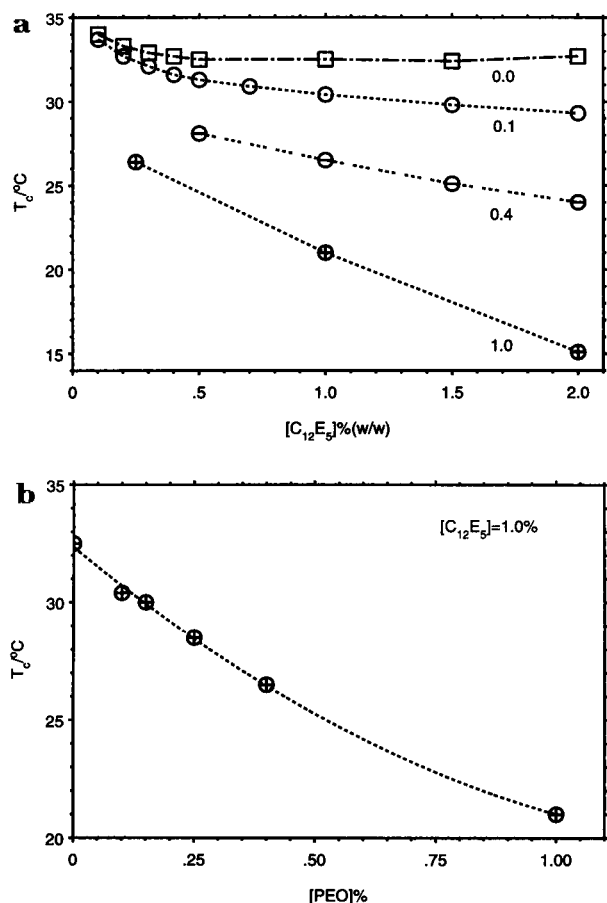


**Figure 13.** (a, top) Clouding temperature ( $T_c$ ) for pure C<sub>12</sub>E<sub>5</sub> and C<sub>12</sub>E<sub>5</sub>/PEO mixtures containing, respectively, PEO at  $c = 0.1$ ,  $0.4$ , and  $1.0\%$ . (b, bottom) Dependence of clouding temperature ( $T_c$ ) on PEO concentration at a constant concentration of C<sub>12</sub>E<sub>5</sub>,  $1\%$ .

constant only changed from  $1.4 \times 10^6$  to  $1.3 \times 10^6$  s<sup>-1</sup> as  $N$  increased from 280 to 380. The dependence of  $k_q$  ( $A_4$ ) on  $N$  is larger in pure surfactant solutions.<sup>30</sup> However, when the polymer is present,  $k_q$  is generally smaller for a given  $N$  than in the absence of polymer.<sup>31–33</sup>

Figure 13a shows how the clouding temperature ( $T_c$ ) for a solution of pure C<sub>12</sub>E<sub>5</sub> in water varies with surfactant concentration and compares these data with the corresponding cloud points for similar solutions containing  $0.1$ ,  $0.4$ , and  $1.0\%$  PEO. We find a value of  $T_c = 32.5$  °C for pure C<sub>12</sub>E<sub>5</sub> at a concentration of  $1\%$ , which is in good agreement with literature values.<sup>11</sup> The addition of PEO to a solution of C<sub>12</sub>E<sub>5</sub> thus decreases  $T_c$  as shown in Figure 13b at an arbitrarily chosen concentration of  $1\%$  C<sub>12</sub>E<sub>5</sub>. The decrease is a strong function of the concentration of PEO. C<sub>12</sub>E<sub>5</sub>/PEO mixtures exhibit a pronounced decrease in  $T_c$  as the PEO concentration is increased at constant surfactant concentration. Above a PEO concentration of  $\sim 1.5\%$ , the solution clouds at room temperature. For equal concentrations of PEO and C<sub>12</sub>E<sub>5</sub> of  $1\%$ ,  $T_c = 21$  °C;  $T_c$  then increases on dilution of the solution. Similar behavior was noted for C<sub>12</sub>E<sub>8</sub> together with PEO<sup>28</sup> and also a hydrophobized PEO sample.<sup>25</sup> These observations support the conclusion of micellar cluster formation within the PEO coil domains. If there had been the type of surfactant/polymer interaction which occurs in PEO/SDS solutions in which small micelles are bound to the polymer chain, one would anticipate that the cloud point would have increased. The interactions between neutral polymers and non-ionic surfactants is a subject of

on-going investigation.

## Conclusions

1. Addition of a low concentration of the non-ionic surfactant C<sub>12</sub>E<sub>5</sub> to binary solutions of high molecular weight PEO inhibits formation of PEO clusters, which are a well-known feature of aqueous solutions of this polymer, by incorporating hydrophobic residues into the micellar core.

2. Above minimum concentrations of C<sub>12</sub>E<sub>5</sub> and PEO, depending on the temperature, the correlation functions are bimodal. The fast component is consistent with the size of the free micelles of surfactant and the slow to the formation of a complex made up of clusters of C<sub>12</sub>E<sub>5</sub> micelles stabilized within the PEO coil. Since the micelles are close to their overlap point, the formation of the latter is promoted by the excluded-volume effect of the high molar mass PEO.

3.  $R_H$  for the PEO/C<sub>12</sub>E<sub>5</sub> complex increases strongly with increasing surfactant concentration from an initial value corresponding to the value for the PEO coil. It is concluded that the polymer chains uncoil progressively as the micellar clusters grow within the coil domain. The interactions between PEO and C<sub>12</sub>E<sub>5</sub> clearly differ in kind from those between a neutral polymer and an ionic surfactant since the interactions are nonspecific, contrasting with the more well-defined entity formed in, for example, the PEO/SDS system, where small charged micelles are disposed along the polymeric backbone to provide optimal contact between the chain and the head group regions of the micelles.

4. Fluorescence quenching measurements show that there is a significant increase in the aggregation number of the C<sub>12</sub>E<sub>5</sub> micelles with increasing PEO concentration. Thus, larger micelles within the domain of the PEO coil are stabilized in the form of clusters by the surrounding polymer segments.

5. As the temperature is increased, the mutual interaction between C<sub>12</sub>E<sub>5</sub> micelles becomes more attractive. The cluster number density/size increase strongly toward the cloud point. The clouding temperature ( $T_c$ ) is found to decrease and to be a strong function of the concentration of added PEO.

**Acknowledgment.** This work has been supported by the Swedish National Board for Technical Development (NUTEK) and the Swedish Technical Research Council (TFR). E.F. thanks the Conselho Nacional de Desenvolvimento Científico e Tecnológico (CNPq) for a stipendium (Grant 201720/93-0).

## References and Notes

- (1) *Interactions of Surfactants with Polymers and Proteins*; Goddard, E. D., Ananthapadmanabhan, K. P., Eds.; CRC Press: Boca Raton, FL, 1993.
- (2) Saito, S. Polymer-surfactant interactions. In *Non-ionic Surfactants*; Schick, M. J., Ed.; Marcel Dekker: New York, 1987.
- (3) Lindman, B.; Thalberg, K. In *Interactions of Surfactants with Polymers and Proteins*; Goddard, E. D., Ananthapadmanabhan, K. P. CRC Press: Boca Raton, FL, 1993.
- (4) (a) Cabane, B. *J. Phys. Chem.* **1977**, *81*, 1639. (b) Cabane, B.; Duplessix, R. *J. Phys. Chem.* **1982**, *43*, 1529.
- (5) Brown, W.; Fundin, J.; da Graça Miguel, M. *Macromolecules* **1992**, *25*, 7192.
- (6) Almgren, M.; Hansson, P.; Mukhtar, E.; van Stam, J. *Langmuir* **1992**, *8*, 2405.
- (7) Brown, W.; Fundin, J. *Macromolecules* **1994**, *27*, 5024.
- (8) (a) Ricka, J.; Meewes, M.; Nyffenegger, R.; Binkert, Th., *Phys. Rev. Lett.* **1990**, *65*, 657. (b) Meewes, M.; Rika, J.; de Silva, M.; Nyffenegger, R.; Binkert, Th. *Macromolecules* **1991**, *24*, 5811.

- (9) Brackman, J. C.; van Os, N. M.; Engberts, J. B. F. M. *Langmuir* **1988**, *4*, 1266.
- (10) Winnik, F. M. *Langmuir* **1990**, *6*, 522.
- (11) Cohen-Addad, S.; di Meglio, J.-M. *Langmuir* **1994**, *10*, 773.
- (12) Sinn, C.; Woermann, D. *Ber. Bunsenges. Phys. Chem.* **1992**, *96*, 913.
- (13) Brown, W.; Zhou, P.; Rymdén, R. *J. Phys. Chem.* **1988**, *92*, 6086.
- (14) Schillén, K.; Brown, W.; Johnsen, R. M. *Macromolecules* **1994**, *27*, 4825.
- (15) Infelta, P. P.; Grätzel, M.; Thomas, J. K. *J. Phys. Chem.* **1974**, *78*, 190.
- (16) Tachiya, M. *Chem. Phys. Lett.* **1975**, *33*, 289.
- (17) Nilsson, P. G.; Wennerström, H.; Lindman, B. *J. Phys. Chem.* **1983**, *87*, 1377.
- (18) Kato, T.; Anzai, S.; Seimiya, T. *J. Phys. Chem.* **1987**, *91*, 4655.
- (19) Brown, W. *Macromolecules* **1984**, *17*, 66.
- (20) Devanand, K.; Selser, J. C. *Macromolecules* **1991**, *24*, 5943.
- (21) Kinugasa, S.; Nakahara, H.; Fudagawa, N.; Koga, Y. *Macromolecules* **1994**, *27*, 6889.
- (22) Burchard, W.; Schmidt, M.; Stockmayer, W. H. *Macromolecules* **1980**, *13*, 1265.
- (23) Rosch, M. In *Non-ionic Surfactants*; Surfactant Science series 1; Schick, M. J., Ed.; Marcell Dekker: New York, 1987; pp 753–793.
- (24) Piculell, L., private communication.
- (25) Alami, E.; Brown, W.; Almgren, M.; Francois, J. *Macromolecules*, in press.
- (26) Wormuth, K. R. *Langmuir* **1991**, *7*, 1622.
- (27) Brown, W.; Mortensen, K. *Macromolecules* **1988**, *21*, 420.
- (28) Feitosa, E.; Brown, W.; Swanson-Vethamuthu, M., submitted to *Macromolecules*.
- (29) Zana, R.; Weill, C. *J. Phys. Lett.* **1985**, *46*, 953.
- (30) Almgren, M. In *Kinetics and Catalysis in Microheterogeneous Systems*, Grätzel, M., Kalyanasundaram, K. Eds.; Marcel Dekker: New York, 1991.
- (31) Zana, R.; Lianos, L.; Lang, J. *J. Phys. Chem.* **1985**, *89*, 41.
- (32) Zana, R.; Binana-Limbelé, W.; Kamenka, N.; Lindman, B. *J. Phys. Chem.* **1992**, *96*, 5461.
- (33) van Stam, J.; Almgren, M.; Lindblad, C. *Progr. Colloid Polym. Sci.* **1991**, *84*, 13.

MA950516G